Indonesian Journal of Maritime Technology (ISMATECH)
Vol. 04, Issue 02, December 2026
eISSN: 3025-518X
DOI: https://doi.org/10.35718/ismatech.v4i2.8482327

Effect of Void and Blister Defects on the Tensile Strength of GFRP Laminates

Restu Muharom[1], Achmad Zubaydi[1], Mohammad Nurul Misbah[1], Rizky Chandra Ariesta[1], Dzaky Hanif Arjuna[2]

[1] Department of Naval Architecture, Faculty of Marine Technology, Institut Teknologi Sepuluh Nopember, Surabaya 60111, Indonesia
[2] Department of Computer Engineering. Faculty of Intelligent Electrical and Informatics Technology, Institut Teknologi Sepuluh Nopember, Surabaya 60111, Indonesia

KEYWORDS
GFRP;
Hand lay-up;
Void;
Blister;
Tensile Strenght

ABSTRACT – Glass fiber reinforced polymer (GFRP) laminates fabricated by hand lay-up are prone to interlaminar defects such as voids and blisters because compaction pressure, resin distribution, and ply alignment depend on operator skill rather than controlled process parameters. This study characterizes the tensile response of hand lay-up chopped strand mat/woven roving (CSM-WR) GFRP laminates with 8, 10, and 12 reinforcement layers, each containing an intentionally introduced interlaminar defect, and compares the results with the minimum tensile strength required by the Indonesian Classification Bureau (BKI) and with published data for related laminate systems. Three specimens were tested per configuration using ISO 527-4 tensile coupons at a crosshead speed of 5 mm/min. All nine specimens exceeded the 98 MPa BKI minimum despite the defects. The mean ultimate tensile strength was 137.59 MPa for the 8 layer group, 118.20 MPa for the 10-layer group, and 137.09 MPa for the 12-layer group, showing that tensile strength did not increase monotonically with layer count, a trend also observed in published hybrid fiber laminates with the same layer counts. The 12 layer group, which carried a blister type defect, had a mean tensile strength about 7% below a published defect free 12 layer CSM-WR benchmark and the highest coefficient of variation (17.72%) among the three configurations, consistent with compaction pressure being a dominant source of scatter in hand lay-up GFRP. These findings indicate that localized void and blister type defects of the size introduced here do not necessarily disqualify hand lay-up CSM-WR panels from meeting BKI tensile strength requirements, though closer control of compaction during lay-up of thicker laminates is warranted.

*Corresponding Author | Achmad Zubaydi | ✉ (zubaydi@its.ac.id)

INTRODUCTION

Glass fiber reinforced polymer (GFRP) is increasingly used in hulls, decks, and other marine structural components because of its high strength to weight ratio, corrosion resistance, and simple fabrication relative to metallic materials [1]. Structural performance, however, depends on laminate design and manufacturing quality as much as on fiber and matrix type [2][3][4]. The fabricated condition of a laminate should therefore be evaluated before GFRP is used as a ship structural component.

In GFRP laminates, the number and arrangement of layers determine the fiber fraction, load transfer directions, thickness, and continuity between layers. Studies of FRP ship materials have shown that fiberglass layer configurations used in shipyards produce measurable differences in strength [5], and tensile testing of fiberglass boat laminates with varying numbers of CSM and WR plies has similarly shown that tensile strength increases with the number of laminate layers [6]. Combinations of chopped strand mat (CSM) and woven roving (WR) have also been investigated as alternative laminates for ship structures because these reinforcements have different roles in carrying loads and maintaining interlaminar bonding [7]. Experiments on glass fiber reinforced polyester show that laminate architecture is directly related to tensile response [8], while different stacking sequences can alter tensile strength even when similar material systems are used [9]. These findings indicate that defect effects should be compared between specimens with equivalent layer counts and stacking arrangements so that any strength reduction is not confounded by the laminate configuration.

Tensile strength is a primary parameter for assessing the ability of a laminate to sustain longitudinal loading before failure. The mechanical properties of glass fiber reinforced polyester composites have been examined through tensile testing to explain the relationship between their constituent materials and failure response [10]. Tensile, compressive, and cyclic tests of GFRP have shown that its behavior is strongly affected by matrix

This is an open access article under the CC BY-SA license.
Copyright © 2026 by Author

cracking, fiber-matrix debonding, and fiber breakage [11]. Agreement between experimental tests and numerical models of polyester-matrix GFRP also demonstrates that tensile data are needed to quantify material capacity [12]. In addition, different matrix materials can produce different tensile and flexural strengths in GFRP systems [13]. Therefore, consistent materials, specimen geometry, and tensile test procedures are required for meaningful comparisons among laminate configurations containing controlled defects.

Hand lay-up remains widely used because it requires simple equipment, has a low initial cost, and can be readily applied to ship components with various shapes. However, its manual nature means that resin thickness, compaction pressure, fiber wetting, and ply alignment depend strongly on operator skill. Different manufacturing techniques have been shown to produce different mechanical properties in glass fiber reinforced polyester composites [14]. Comparisons of hand lay-up, vacuum bagging, and vacuum infusion also show that the fabrication method affects laminate quality and tensile properties [15]. Although infusion processes provide better control of resin flow and compaction, incomplete filling remains possible [16], [17]. In hand lay-up, limited control of pressure and resin distribution increases the risk of resin rich regions, incomplete fiber wetting, voids, and local interlaminar separation.

In addition to the manufacturing method, the tensile response of GFRP is affected by fiber fraction, orientation, thickness, and stacking sequence. Composite mechanics principles indicate that changes in the relative contributions of the fibers and matrix alter the tensile modulus and strength of a laminate [18]. Tests of different fiber configurations and thicknesses have shown variations in tensile behavior, including after exposure to elevated temperatures [19] or harsh environments [20]. The stacking sequence also affects interlaminar shear strength and susceptibility to failure between layers [21]. Consequently, the mechanical response of defect containing laminates should be interpreted by considering the layer configuration, laminate architecture, and actual specimen dimensions.

A void is an empty region formed when trapped air or gas is not fully displaced by resin during lamination and curing. Voids may result from uneven wetting, resin viscosity, mixing, or insufficient compaction. A review of voids in fiber reinforced composites explains that their size, shape, location, and quantity govern the extent to which they disrupt stress transfer paths [22]. Reviews of manufacturing defects also identify voids, delamination, fiber waviness, and resin rich or resin starved regions as sources of reduced composite quality [23]. Because void content can be determined using destructive and nondestructive methods [24], it should be treated as a measurable variable and related directly to changes in mechanical properties, rather than considered only a visual imperfection.

Mechanically, voids reduce the effective load bearing area, disrupt fiber matrix bonding, and create stress concentrations that can initiate cracks. Porosity detection studies on GFRP have shown that internal defect distributions can be identified and distinguished from more homogeneous regions of a laminate [25]. Acoustic-emission analyses of GFRP damage mechanisms have shown that matrix cracking, debonding, delamination, and fiber breakage can develop progressively during loading [26]. For ship design, increasing void content has been reported to reduce the mechanical properties of GFRP laminates [27]. These findings suggest that specimens containing defects may fail earlier than defect-free specimens even when both have the same nominal number of layers.

A blister is a local bulge or bubble associated with layer separation, fluid or air accumulation, or osmotic pressure within a laminate. In FRP structures exposed to seawater, critical blister size has been associated with reduced load carrying capacity after ageing [28]. Research on the interaction of void content, moisture uptake, and mechanical strength also indicates that initial defects can accelerate moisture ingress and weaken the fiber matrix interface [29]. Delamination detection methods for GFRP enable quantitative mapping of local defects [30], while recent micromechanical analyses confirm that void content, size, and shape have distinct effects on composite strength and ductility [31]. Therefore, voids and blisters should be evaluated as different defect types with different failure mechanisms.

Previous studies have examined layer configurations, manufacturing methods, void content, interlaminar damage, and defect-detection techniques. Nevertheless, experimental data on the tensile response of marine hand lay-up CSM-WR/polyester laminates containing intentionally introduced interlaminar defects across multiple layer configurations remain limited. Several studies have evaluated defects through nondestructive inspection or modeling; however, fewer studies report the measured tensile strength, specimen to specimen variability, and failure behavior of severe controlled defect regions in 8, 10, and 12 layer laminates fabricated and tested under the same procedure. This limitation defines the research gap addressed in the present study.

When the number of layers is considered specifically, Zakki and Windyandari [8] provide the closest reference for the 8 layer laminate because their study used GFRP, Yukalac polyester resin, hand lay-up, and tensile testing. For the 10 layer configuration, Beng et al. [32] used EWR-600 woven E-glass and polyester resin, fabricated by hand lay-up, to evaluate Mode I delamination. Their study is relevant to interlaminar damage but did not measure tensile strength. For the 12-layer configuration, Ma'ruf et al. [7] investigated CSM-WR/polyester laminates for ship structures and reported a mean tensile strength of 147.8 MPa. Dawood et al. [33] used the same layer counts of 8, 10, and 12 and conducted tensile and flexural tests; however, their specimens consisted of glass carbon hybrid fibers, an epoxy matrix, an infusion process, and added SiO2 nanoparticles. Their study is therefore useful for structuring the presentation of layer-count variations but is not a direct experimental comparator. Taking together, these studies do not provide a directly comparable tensile evaluation of hand lay-up 8, 10, and 12 layer CSM-WR/polyester laminates containing intentionally introduced void and blister type interlaminar defects.

Numerical studies of damaged fiberglass ship structures have identified representing defect conditions close to those actually observed in service, rather than idealized laboratory geometries, as a persistent challenge in evaluating structural response, and have specifically flagged blister type damage as among the most failure prone conditions for fiberglass hulls [34]. The scientific novelty of the present study is that the void and blister type defects were intentionally shaped to approximate this in service damage morphology, rather than using simplified or arbitrary defect geometries, so that the resulting tensile data are more directly relevant to laminates already exhibiting field like degradation. This study aims to characterize the tensile response of hand lay-up GFRP laminates containing such intentionally introduced, field-representative interlaminar defects. Laminates with 8, 10, and 12 reinforcement layers were fabricated and tested using the same tensile-test procedure. The ultimate tensile strength, specimen to specimen variability, and visual failure characteristics of each configuration were evaluated using the actual measured cross sectional dimensions. The mean tensile strengths were also compared with the minimum requirement of 98 MPa specified by the Indonesian Classification Bureau. The resulting data set provides an experimental basis for evaluating the performance of defect containing GFRP laminates used in ship structures.

This study has two related limitations. First, no numerical model of the defect containing laminates was developed to validate the tensile-test results against a predicted stress response. Building such a model is itself difficult because the irregular, field like void and blister geometries used here cannot be represented exactly in a finite element mesh a numerical representation could only approximate them using simplified idealized shapes, as Triwilaswandio et al. [34] did when modeling ship damage as cracks, holes, and blisters of prescribed depth rather than the irregular geometries actually observed in service. Second, the size and position of the defect in each panel were fixed by the fabrication procedure rather than randomized across replicate specimens, so the reported specimen to specimen scatter reflects both ordinary material variability and this fixed defect placement. These limitations should be considered when generalizing the present tensile results to other defect geometries, sizes, or laminate thicknesses.

METHODS

Constituent Materials and Laminate Lay-up

A laboratory tensile testing program was conducted to characterize GFRP laminates containing deliberately introduced interlaminar defects. The experimental program comprised 8, 10, and 12 ply laminate configurations. Three tensile specimens were tested for each configuration, resulting in a total of nine tests. Because every laminate panel contained an artificial defect, the results were compared among the three defect containing configurations and against the minimum tensile-strength requirement specified by the Indonesian Classification Bureau (BKI) [35]. No defect free control laminates were fabricated.

The glass fiber reinforcement consisted of two chopped strand mats, CSM 300 and CSM 450, and two woven rovings, WR 600 and WR 800. The numerical designations indicate the nominal areal mass of each reinforcement. Accordingly, CSM 300, CSM 450, WR 600, and WR 800 have nominal areal masses of 300, 450, 600, and 800 g/m², respectively [5], [7], [34]. CSM consists of discontinuous glass strands randomly distributed and oriented within the laminate plane, whereas WR consists of continuous roving bundles woven in the warp and weft directions [6]. This structural difference is reflected in their damage behavior under cyclic tension, where CSM and WR composites have been shown to fail through distinct mechanisms [39]. The dry glass fiber reinforcements used in this study are shown in Figure 1.

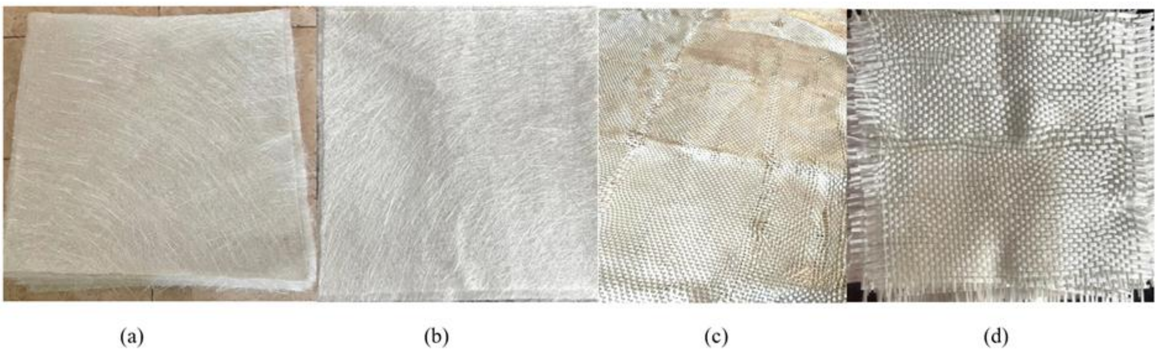

Figure 1. Dry glass-fiber reinforcements used in laminate fabrication: (a) CSM 300 (300 g/m²), (b) CSM 450 (450 g/m²), (c) WR 600 (600 g/m²), and (d) WR 800 (800 g/m²).

The stacking sequences adopted for the three laminate configurations are presented in Table 1. Each configuration consisted of alternating CSM and WR reinforcements, with variations in the number and arrangement of plies. These differences were considered in evaluating the influence of laminate configuration on the observed tensile behavior.

Table 1. Ply arrangements of the investigated laminates.

Code	Stacking sequence
L8	CSM 300 / CSM 450 / WR 600 / WR 800 / WR 600 / CSM 450 / WR 600 / CSM 300
L10	CSM 300 / CSM 450 / WR 600 / WR 800 / WR 600 / CSM 450 / WR 600 / CSM 450 / WR 600 / CSM300
L12	CSM 300 / CSM 450 / WR 600 / WR 800 / WR 600 / CSM 450 / WR 600 / CSM 450 / WR 600 / CSM 450 / WR 600 / CSM 300

The laminate panels were fabricated by hand lay-up using a flat 300 × 300 mm open mold [8]. Before fabrication, the mold surface was cleaned and coated uniformly with release wax. Yulkalac-157 unsaturated polyester resin was used as the matrix, while Mexpone was added at 1 vol% as the curing catalyst [40]. For each panel, 2,000 ml of resin was mixed gently with 20 ml of Mexpone for approximately 1 min. The reinforcement sheets were then cut to match the mold dimensions and arranged according to the specified stacking sequence. Resin was applied manually to each reinforcement layer, followed by rolling to improve impregnation and remove unintended entrapped air [41]. The materials used for mold preparation and resin mixing are shown in Figure 2.

(a) (b) (c)

Figure 2. Materials employed in panel production (a) release wax, (b) Yulkalac-157 resin and (c) addition of Mexpone catalyst.

The artificial defect was introduced during placement of the final three plies. In a central zone approximately 50 mm wide, part of the reinforcement was lifted and compacted less than the adjacent laminate. This treatment trapped air within the near-surface interfaces while leaving the remaining laminate thickness continuous. The defect zone extended nominally across the 300 mm panel width and was oriented transverse to the direction of tensile loading.

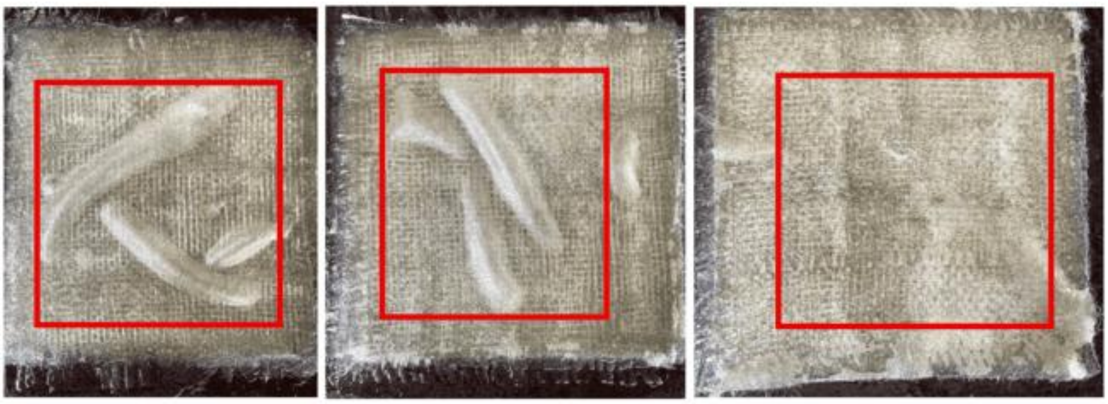

(a) (b) (c)

Figure 3. Visual appearance of the intentionally introduced interlaminar defects in the GFRP laminates: (a) 8 layer laminate with a void type of defect, (b) 10 layer laminate with a void type of defect, and (c) 12 layer laminate with void and blister type defect.

The same defect forming procedure was followed for all three lay-ups. However, the manual process produced visible differences in the geometry and distribution of the defective regions. Because of surface appearance, the defects in the 8 and 10 ply panels were described as void type, whereas the defect in the 12 ply panel was described as blister type (Figure 3). This terminology represents a visual classification only, since no nondestructive examination was performed to confirm the internal morphology. The completed panels were cured for 24 hours at ambient room conditions. Temperature and relative humidity were not controlled or recorded.

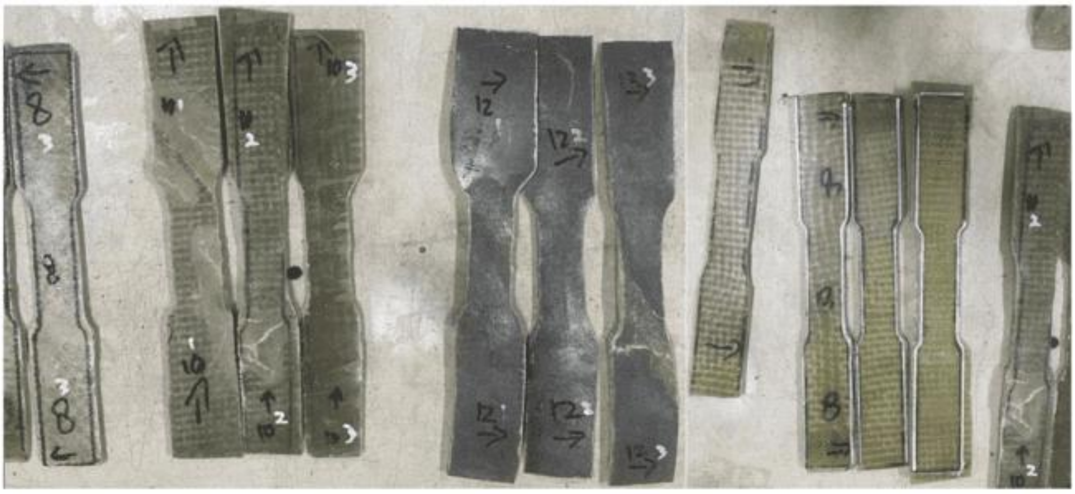

(a) (b) (c)

Figure 4. Tensile specimens cut from the cured laminates: (a) 8 layer, (b) 10 layer, and (c) 12 layer specimen groups.

After curing, the panels were demolded and cut into tensile specimens with the selected ISO 527-4 geometry [36], [37]. Three specimens were prepared from each laminate configuration. The resulting 8, 10, and 12 ply specimen groups are shown in Figure 4.

Tensile Test Procedure

Three tensile specimens were prepared from each laminate configuration. The specimens were cut from the laminated panels according to the geometry specified in ISO 527-4 [37], as shown in Figure 5. As defined in Figure 5, each specimen had a total length of 300 mm, a nominal reduced section width of 30 mm, a transition radius of 60 mm, a grip section length of 60 mm, and an initial gauge length of 50 mm. The width and thickness of each specimen were measured before testing, and the initial cross sectional area was calculated using Equation (1). Tensile tests were subsequently conducted at a constant crosshead speed of 5 mm/min in accordance with ISO 527-1 and ISO 527-4 [36], [37]. The BKI requirement was used as the acceptance criterion for evaluating the tensile strength results [35]. For each laminate configuration, the results were reported as the mean and standard deviation of three replicate specimens [5].

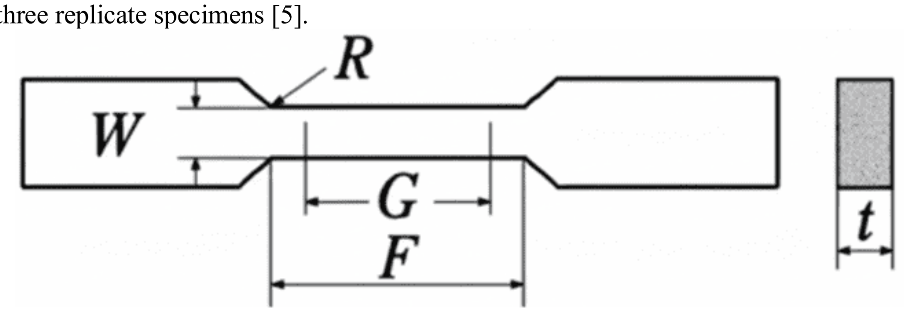

Figure 5. Tensile coupon profile and dimensional notation.

Tensile testing plays an important role in evaluating the mechanical performance of composite materials by determining parameters such as tensile strength, elastic modulus, elongation, and fracture behavior. Each specimen is subjected to tensile loading until failure, while the corresponding load and deformation data are recorded throughout the test. The results describe the material response under tensile loading and provide essential information for the design and engineering of plastic- and composite based products [35].

Figure 6. GFRP tensile specimen mounted in the universal testing machine.

$$A_0 = \omega \times t \qquad (1)$$

Where A_0 is the initial cross sectional area (mm^2), w is the measured specimen width (mm), and t is the measured specimen thickness (mm).

Table 2. BKI Rules for Fiberglass

A	Tensile Strength	10	kg/mm^2
B	Modulus Of Tensile Elasticity	700	kg/mm^2

The relevant requirements of the Indonesian Classification Bureau (BKI) are summarized in Table 2. The regulations governing the testing of fiberglass vessels are specified in the Rules for fiber reinforced plastic (FRP) Ships, particularly part 1: general regulations, section C: general requirements for hull structures and equipment, item 4 scantlings. These requirements apply to FRP structures manufactured using glass fiber reinforcement with unsaturated polyester or epoxy resin through hand lay-up or spray-up lamination. Fiberglass reinforced materials incorporating hybrid or roving reinforcements must satisfy the specified minimum strength requirements [35].

$$Xmin = a\left[Xref\left(\frac{\varphi}{0.4}\right)\right] - [1278\varphi^2 + 510\varphi + 123]MPa \qquad (2)$$

The minimum strength is governed by several factors, including the intrinsic material property represented by $Xref$, the parameter φ, and several empirical constants. $Xmin$ represents the minimum allowable value of the evaluated property, such as the minimum tensile strength $Xref$ serves as the reference value, while variations in φ affect the resulting value of $Xmin$. The constants (a), (b), (c), and (d) are empirical coefficients used to fit the equation to experimental data. The constant 0.4 is used to normalize φ within the applicable range. Overall, the equation describes the relationship among the parameters that influence the minimum strength of the material.

In this study, the fiber volume fraction φ is considered an important parameter affecting material performance. A fiber volume fraction of 0.30, or 30%, was adopted to represent the laminate composition of the specimens. The required minimum strength $Xmin$ is expressed in MPa. The reference strength $Xref$ was set at 500 MPa for tensile strength. The orientation factor a was also included to account for the orientation of the reinforcing fibers. For tensile and flexural loading with a 0°/90° fiber orientation, a was assigned a value of 0.55. The experimental data were subsequently used to determine the strain, stress, elastic modulus, and maximum stress of each specimen.

Tensile strain represents the change in specimen length relative to its initial length during tensile testing [38]. It was calculated using the following equation:

$$\varepsilon = \frac{\Delta L}{Lo} \tag{3}$$

Where ε is the tensile strain, ΔL is the change in specimen length before and after loading (mm), and Lo is the initial specimen length (mm). Using this equation, the tensile strain was calculated to quantify the deformation of the material under the applied tensile load.

RESULTS AND DISCUSSION

This section presents and discusses the tensile-test results of the 8, 10, and 12-layer GFRP specimens containing intentionally introduced defects. The discussion focuses on ultimate tensile strength, tensile strain, and observed fracture characteristics to evaluate the effects of laminate configuration and defects on mechanical performance.

Each specimen was mounted in a universal testing machine and loaded to failure the fractured specimens are shown in Figure 7.

(a) (b) (c)

Figure 7. Fractured GFRP tensile specimens after testing, with the fracture zone highlighted: (a) 8 layer, (b) 10 layer, and (c) 12 layer specimen.

The results are also assessed against the minimum requirements of Biro Klasifikasi Indonesia (BKI) and compared with relevant published data for nominally defect free laminates.

Table 3. Ultimate tensile strength of GFRP specimens by laminate configuration

Specimen Code	Configuration	Ultimate Stress (MPa)
A	8-layer	149.84
B	8-layer	140.48
C	8-layer	122.45
D	10-layer	114.93
E	10-layer	122.37
F	10-layer	117.30
G	12-layer	147.77
H	12-layer	109.29
I	12-layer	154.21

The specimen was clamped at both grip sections and loaded in tension at a constant crosshead speed of 5 mm/min until fracture, with load and crosshead displacement recorded throughout the test for subsequent calculation of stress and strain.

Visually, the fracture location in all three configurations fell within or adjacent to the defect zone marked in Figure 7, but the photographs alone are not sufficient to establish that cracking always initiated at the void or blister. In the 8 layer (void) specimens, fracture surfaces show fiber breakage, fiber pull-out, and localized interlaminar separation, with the fracture location varying between specimens, consistent with a non-uniform distribution of void content or impregnation quality across the panel. In the 10 layer (void) specimens, damage is dominated by broken fiber bundles and pulled out fibers, and the fracture plane again did not form at a single consistent position this configuration nevertheless produced the most uniform mechanical results of the three, although this does not by itself imply a smaller void effect.

All nine specimens exceeded the 98 MPa minimum tensile strength required by the Indonesian Classification Bureau (BKI) despite the intentionally introduced interlaminar defects, as shown in Figure 8. The mean ultimate tensile strength was 137.59 MPa for the 8 layer group, 118.20 MPa for the 10 layer group, and 137.09 MPa for the 12 layer group, so the 10 layer configuration in this study consistently returned the lowest strength of the three, while the 8 and 12 layer groups performed similarly to one another.

The absence of a monotonic increase in strength with layer count is consistent with results reported for other hand-fabricated GFRP systems. Dawood et al. [33] tested glass/carbon hybrid laminates with the same 8, 10, and 12 layer arrangement and likewise found that tensile stress did not increase steadily with layer number, recording 374.05 MPa, 399.97 MPa, and 352.14 MPa for their 8, 10, and 12 layer laminates, respectively, even though those laminates were produced by resin infusion rather than hand lay-up. This suggests that layer count alone is not a reliable predictor of tensile strength across studies, and that stacking sequence and fabrication consistency play at least as large a role as ply count.

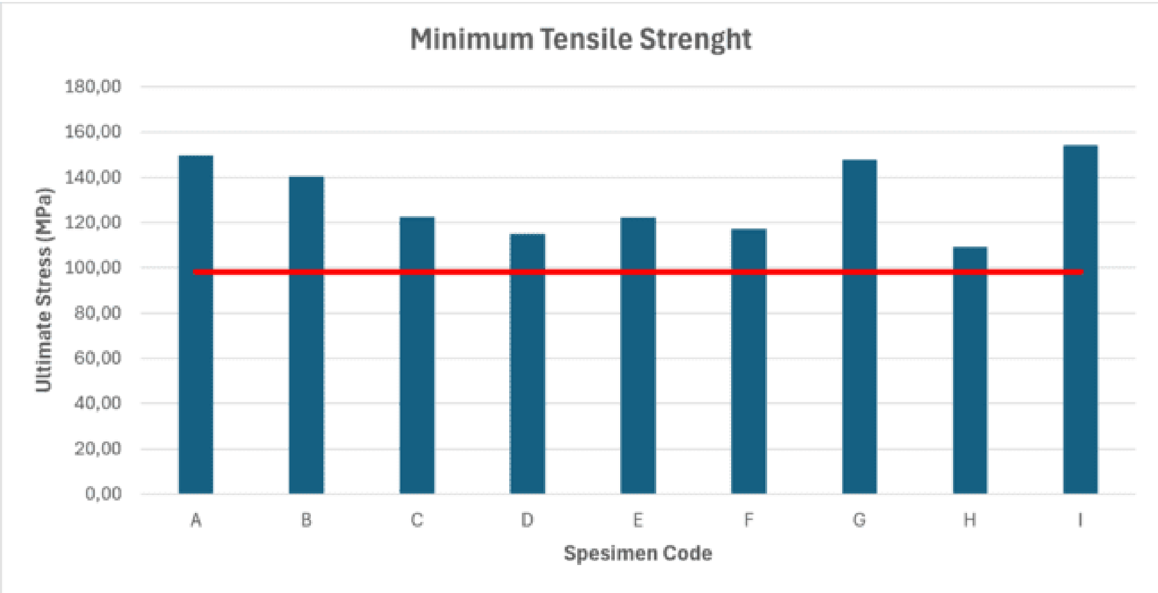

Figure 8. Ultimate tensile stress of GFRP specimen (A–I) compared with the BKI minimum tensile strength**.**

The tensile response of the 8 layer laminate configuration was evaluated from the stress–strain curves of specimens A–C, as presented in Figure 9. The curves provide a comparison of the deformation behavior and ultimate tensile stress among the three specimens containing intentionally introduced void type defects.

All three curves follow a similar shape a near linear region up to approximately 0.002 strain, a transitional region of reduced stiffness between 0.002 and 0.004 strain, and a final near linear rise to failure. Specimens A and B reached the highest ultimate stresses (149.84 MPa and 140.48 MPa), while Specimen C failed at a visibly lower stress (122.45 MPa) despite tracking an almost identical curve up to about 0.003 strain, indicating that the difference in ultimate strength emerged mainly in the later loading stage rather than in the initial elastic response.

The tensile response of the 10 layer laminate configuration was assessed using the stress–strain curves of specimens D–F, as shown in Figure 10. These curves allow the deformation behavior and ultimate tensile stress of the three specimens containing intentionally introduced void type defects to be compared.

The three curves remain closely grouped throughout the test, consistent with the low 3.22% coefficient of variation already reported for this configuration. None of the three specimens exceeded approximately 122 MPa, and the curves diverge only slightly near final failure, indicating that the 10-layer laminates behaved more uniformly under load than the 8 or 12 layer groups.

The experimental results show that the ultimate tensile stress fluctuated in direct association with the laminate thickness, i.e., the number of layers. The 8-layer configuration (specimens A-C) demonstrated the highest mechanical stability, with ultimate stress ranging from 122.45 to 149.84 MPa. In contrast, the added thickness of the 10 layer configuration (specimens D-F) paradoxically induced a reduction in load carrying capacity, with recorded ultimate stresses falling in the narrower range of 114.93-122.37 MPa. The 12 layer configuration (specimens G-I) then showed an extreme standard deviation, with stress values fluctuating sharply and asymmetrically between a low of 109.29 MPa and a high of 154.21 MPa. This anomalous drop and instability in the thicker specimens can be explained in more depth through a macroscopic analysis of the failure mode of each specimen.

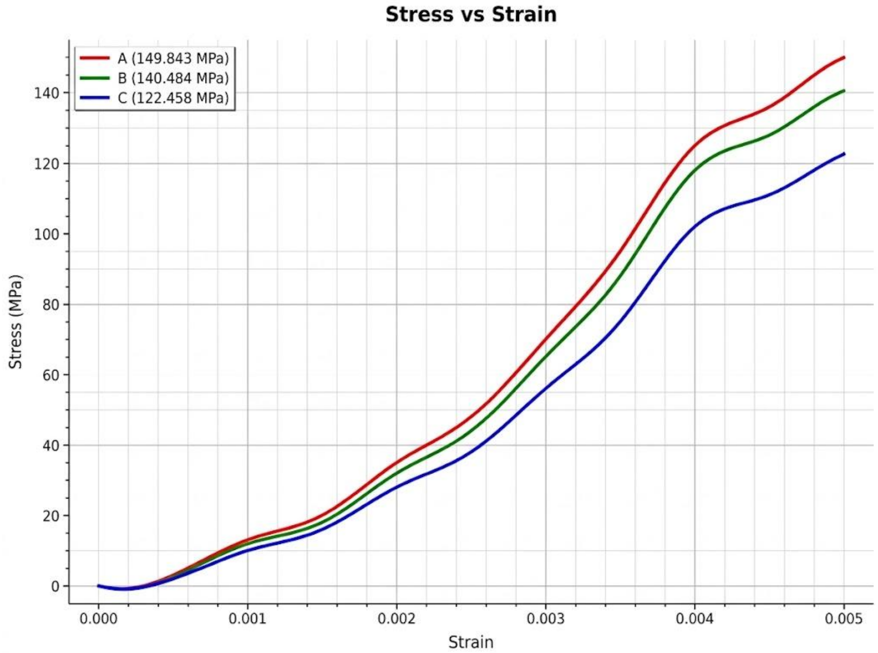

Figure 9. Stress-strain response of the 8 layer GFRP specimen (A-C).

Visual evaluation of the fracture area confirms a transition in failure mode as the number of laminae increases. In the 8 layer composite (Figure 7a), transverse fracture is concentrated precisely within the gauge length. Failure in this group is dominated by fiber breakage with minimal secondary delamination. This clean fracture morphology indicates that mechanical stress transfer from the matrix to the reinforcing fibers proceeded effectively, allowing the specimens to reach their maximum axial capacity before total structural failure. In the 10 layer configuration (Figure 7b), the macroscopic fracture profile transitions to an asymmetric, jagged form. Structural failure in these specimens is visually characterized by fiber pull out together with extensive longitudinal delamination. This degradation of interlaminar cohesion represents a premature failure mechanism, in which the matrix bond had already failed before the axial tensile stress on the fibers reached its maximum value, which rationally explains the reduced ultimate stress observed for the 10 layer configuration.

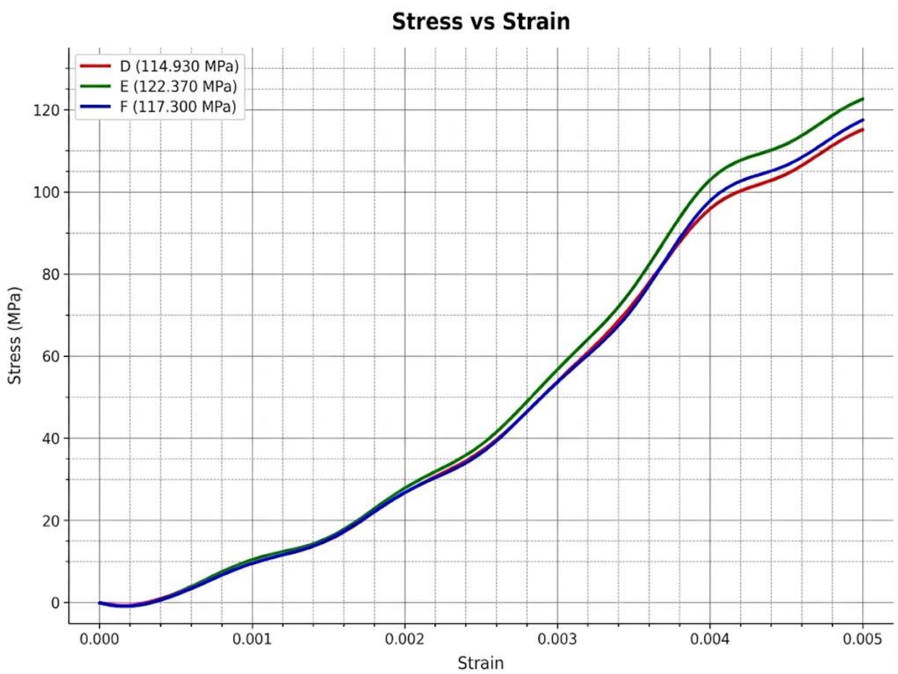

Figure 10. Stress-strain response of the 10 layer GFRP specimen (D-F).

In the 12 layer specimens, which combined void content with a localized blister, the blister introduces a failure mechanism not dominantly present in the 8 and 10 layer groups. While the void primarily represents a cavity or a region of incomplete impregnation, the blister resembles a local lifting of near surface ply groups caused by local interfacial separation. A blister of this type can reduce the bonded interlaminar area, alter local thickness, induce fiber waviness, introduce eccentricity into the load path, and increase interlaminar shear and normal stresses at the blister edge. Abd-Elhady et al. [28] found that the size, depth, and geometry of a blister type defect affect the stress concentration and strength of GFRP, and that for relatively small surface defects, delamination plays an important role in damage progression, this supports the view that not only the presence of a blister, but also its position and dimensions, governs the degree of strength reduction. This is consistent with the spread of the 12 layer results. Specimens G and I reached 147.77 and 154.21 MPa, whereas Specimen H reached only 109.29 MPa. This difference could arise if Specimen H intersected a wider or deeper blister or void, or one with greater waviness, whereas in Specimens G and I the defect region may not have severed the main fiber bundles, allowing continuous fibers to retain the load path. It should be noted that Abd-Elhady et al. [28] examined aged GFRP pipes with surface defects used to simulate blistering, so that study supports the proposed mechanism rather than serving as a direct benchmark for the 12 layer strength values reported here. The stress-strain curves of the three 12 layer specimen (G-I) are shown in Figure 11.

For the 12 layer configuration specifically, the present mean of 137.09 MPa is comparable to, though about 7% below, the 147.8 MPa reported by Ma'ruf et al. [7] for a 12 layer CSM-WR/polyester marine laminate fabricated by hand lay-up and evaluated against BKI criteria. Because the present 12 layer panel carried an intentionally formed blister type defect while the Ma'ruf et al. specimens were not reported to contain a deliberate defect, this gap is consistent with a strength penalty from the blister defect, although the 17.72% coefficient of variation within the present 12 layer group, the highest of the three configurations, indicates that specimen to specimen differences in local compaction were also contributing to the scatter.

This interpretation is consistent with the interlaminar fracture study of Beng et al. [32], who found that curing pressure was a more influential controlling parameter for the Mode-I interlaminar fracture toughness of hand lay-up woven GFRP than fiber weight fraction. Because compaction pressure during hand lay-up in the present study depended on manual rolling and was not measured or controlled, local variation in compaction is a plausible source of both the elevated scatter in the 12 layer group and the visual distinction drawn in the Methods between the void type defects observed in the 8 and 10 layer panels and the blister type defect observed in the 12 layer panel.

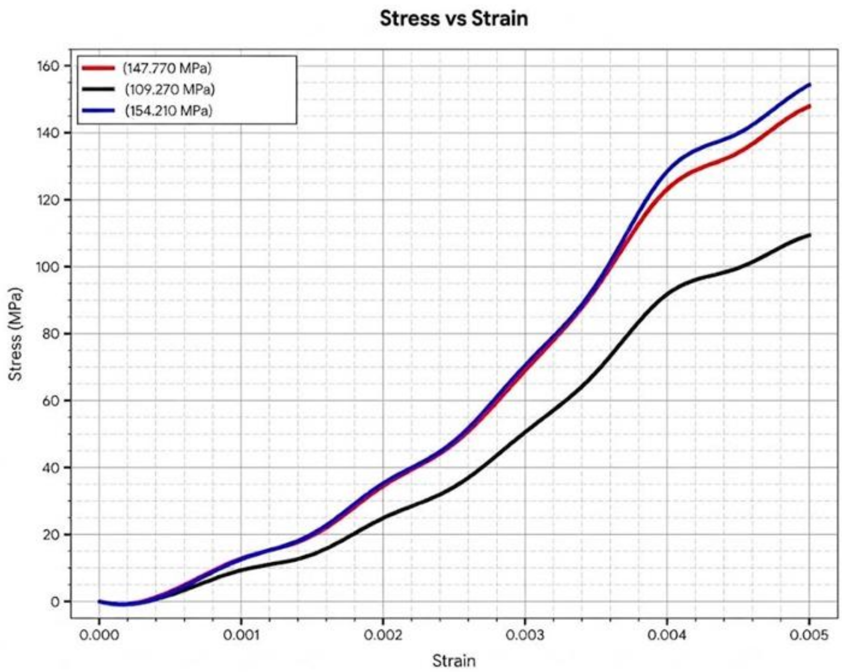

Figure 11. Stress-strain response of the 12 layer GFRP specimen (G-I).

Taken together, the comparison against Dawood et al. [33], Ma'ruf et al. [7], and Beng et al. [32] indicates that the present 8 and 12 layer groups performed in line with, or only modestly below, published defect free or hybrid benchmarks at the same layer counts, while the 10 layer group underperformed both its own 8 and 12 layer counterparts and the corresponding trend in Dawood et al. [33]. This points to the 10-layer panel, and the compaction quality achieved for it, as the configuration most affected by the introduced defect and by hand lay-up variability in this study.

Notwithstanding the absence of a defect free control specimen in the present study, the practical finding for shipyard practice is that hand lay-up CSM-WR panels containing localized void or blister type defects of the size introduced here remained above the BKI minimum tensile strength requirement across all three layer configurations. This indicates that defects of this scale do not necessarily disqualify a panel from meeting classification requirements, although the lower mean and higher variability of the 10 and 12 layer groups relative to the defect free CSM-WR benchmark of Ma'ruf et al. [7] warrant closer quality control of compaction during hand lay-up of thicker laminates.

CONCLUSION

This study characterized the tensile response of hand lay-up CSM-WR GFRP laminates with 8, 10, and 12 reinforcement layers, each containing an intentionally introduced void or blister type interlaminar defect and evaluated the results against the BKI minimum tensile strength requirement and against relevant published data. All nine tested specimens exceeded the 98 MPa BKI minimum, with mean ultimate tensile strengths of 137.59 MPa, 118.20 MPa, and 137.09 MPa for the 8, 10, and 12 layer configurations, respectively. Tensile strength did not increase monotonically with layer count, a pattern consistent with published hand fabricated and hybrid GFRP laminates of the same layer counts, indicating that stacking sequence and fabrication consistency influence tensile strength at least as much as ply count. The 12 layer group, which carried the blister type defect, returned both the highest scatter (17.72% coefficient of variation) and a mean about 7% below a published defect free 12 layer CSM-WR benchmark, pointing to compaction pressure during hand lay-up as a plausible source of the reduced and more variable performance. The practical implication for shipyard practice is that localized void and blister type defects of the size introduced in this study do not necessarily disqualify a hand lay-up CSM-WR panel from meeting BKI tensile strength requirements, although closer quality control of compaction is warranted for thicker laminates. In addition, a void type defect was intentionally introduced in all three configurations, but the 12 layer panel also developed an unintended blister during fabrication consequently, the 12 layer results reflect the combined effect of layer count, the intended void, and this additional blister, and the individual contribution of the blister could not be isolated from the present dataset. Because no defect free control specimen of matching configuration was fabricated in this study, the reduction in tensile strength directly attributable to the void or blister defect could not be isolated from the effects of layer count and ordinary specimen to specimen variability. Future work should therefore fabricate matched intact and defective specimens across the same layer configurations, together with nondestructive evaluation of defect morphology, to quantify the strength penalty of void and blister defects in marine grade GFRP laminates.

REFERENCES

[1] F. Rubino, A. Nistico, F. Tucci, and P. Carlone, "Marine application of fiber reinforced composites: A review," Journal of Marine Science and Engineering, vol. 8, no. 1, art. 26, 2020, doi: 10.3390/jmse8010026.

[2] L. Wijewickrama, J. Jeewantha, G. I. P. Perera, O. Alajarmeh, and J. Epaarachchi, "Fiber-reinforced composites used in the manufacture of marine decks: A review," Polymers, vol. 17, no. 17, art. 2345, 2025, doi: 10.3390/polym17172345.

[3] A. Dinita et al., "Advancements in fiber-reinforced polymer composites: A comprehensive analysis," Polymers, vol. 16, no. 1, art. 2, 2024, doi: 10.3390/polym16010002.

[4] S. Mahboubizadeh, A. Sadeq, Z. Arzaqi, O. Ashkani, and M. Samadoghli, "Advancements in fiber-reinforced polymer (FRP) composites: An extensive review," Discover Materials, vol. 4, no. 1, 2024, doi: 10.1007/s43939-024-00091-9.

[5] A. Ismail, B. Ma'ruf, A. Zubaydi, M. A. D. Octavanny, and T. L. Ginta, "Strength assessment of fiberglass layer configurations in FRP ship materials from yard practices using a statistical approach," Curved and Layered Structures, vol. 11, no. 1, 2024, doi: 10.1515/cls-2024-0007.

[6] R. Ruzuqi, “Tensile strength analysis of polymer composite materials fiber reinforced in the fiberboat application,” Journal of Research and Opinion, vol. 7, no. 8, pp. 2763–2769, 2020, doi: 10.15520/jro.v7i8.74.

[7] B. Ma'ruf, A. Ismail, D. P. Sari, and S. H. Sujiatanti, "Strength analysis of marine biaxial warp-knitted glass fabrics as composite laminations for ship material," Curved and Layered Structures, vol. 10, no. 1, 2023, doi: 10.1515/cls-2022-0209.

[8] A. F. Zakki and A. Windyandari, "Simplified FE model and experimental study on the tensile properties of the glass fiber reinforced polyester polymer," Heliyon, vol. 8, no. 10, art. e10999, 2022, doi: 10.1016/j.heliyon.2022.e10999.

[9] R. Ramli, A. Alisibramulisi, S. M. Noor, and D. D. Suharso, "Analysis of tensile strength on various layer stack sequence of fiber reinforced polymer (FRP)," Journal of Sustainable Civil Engineering and Technology, vol. 1, no. 1, pp. 50-60, 2022, doi: 10.24191/jscet.v1i1.50-60.

[10] I. Milosan, T. Bedo, C. Gabor, and M. A. Pop, "Mechanical characteristics of glass-fiber-reinforced polyester composite materials," Materials, vol. 18, no. 15, art. 3595, 2025, doi: 10.3390/ma18153595.

[11] M. D. Stanciu, H. T. Draghicescu, and I. C. Rosca, "Mechanical properties of GFRPs exposed to tensile, compression and tensile-tensile cyclic tests," Polymers, vol. 13, no. 6, art. 898, 2021, doi: 10.3390/polym13060898.

[12] C. O. Ndukwe, B. O. Ezurike, and P. C. Okpala, "Comparative studies of experimental and numerical evaluation of tensile properties of glass fibre reinforced polyester (GFRP) matrix," Heliyon, vol. 7, no. 5, art. e06887, 2021, doi: 10.1016/j.heliyon.2021.e06887.

[13] A. B. Sulistyo and W. A. Wirawan, "Evaluation of tensile strength and flexural strength of GFRP composites in different types of matrix polymers," Journal of Achievements in Materials and Manufacturing Engineering, vol. 123, no. 1, 2024, doi: 10.5604/01.3001.0054.6847.

[14] G. S. C. Assuncao, J. A. Velasques, A. Zakrzevski, and I. de Costa, "Mechanical properties of glass-fiber reinforced polyester composites manufactured by two different spray-up techniques," Materia (Rio de Janeiro), vol. 29, no. 3, 2024, doi: 10.1590/1517-7076-RMAT-2024-0450.

[15] A. Talabari, M. Alaei, and H. Shalian, "Experimental investigation of tensile properties in a glass/epoxy sample manufactured by vacuum infusion, vacuum bag and hand layup process," Revue des Composites et des Materiaux Avances, vol. 29, no. 3, pp. 179-182, 2019, doi: 10.18280/rcma.290308.

[16] A. Hindersmann, "Confusion about infusion: An overview of infusion processes," Composites Part A: Applied Science and Manufacturing, vol. 126, art. 105583, 2019, doi: 10.1016/j.compositesa.2019.105583.

[17] S. van Oosterom, T. Allen, M. Battley, and S. Bickerton, "An objective comparison of common vacuum assisted resin infusion processes," Composites Part A: Applied Science and Manufacturing, vol. 125, art. 105528, 2019, doi: 10.1016/j.compositesa.2019.105528.

[18] T. I. Altanopoulos and I. G. Raftoyiannis, "Deriving tensile properties of glass fiber reinforced polymers (GFRP) using mechanics of composite materials," Open Journal of Composite Materials, vol. 10, no. 1, pp. 1-14, 2020, doi: 10.4236/ojcm.2020.101001.

[19] A. Jafari et al., "Effect of fibers configuration and thickness on tensile behavior of GFRP laminates subjected to elevated temperatures," Construction and Building Materials, vol. 202, pp. 189-207, 2019, doi: 10.1016/j.conbuildmat.2019.01.003.

[20] M. Bazli, H. Ashrafi, A. Jafari, X.-L. Zhao, R. K. S. Raman, and Y. Bai, "Effect of fibers configuration and thickness on tensile behavior of GFRP laminates exposed to harsh environment," Polymers, vol. 11, no. 9, art. 1401, 2019, doi: 10.3390/polym11091401.

[21] V. Modi, K. K. Singh, and R. Shrivastava, "Effect of stacking sequence on interlaminar shear strength of multidirectional GFRP laminates," Materials Today: Proceedings, vol. 22, pp. 2207-2214, 2020, doi: 10.1016/j.matpr.2020.03.301.

[22] M. Mehdikhani, L. Gorbatikh, I. Verpoest, and S. V. Lomov, "Voids in fiber-reinforced polymer composites: A review on their formation, characteristics, and effects on mechanical performance," Journal of Composite Materials, vol. 53, no. 12, pp. 1579-1669, 2019, doi: 10.1177/0021998318772152.

[23] Y. Fu and X. Yao, "A review on manufacturing defects and their detection of fiber reinforced resin matrix composites," Composites Part C: Open Access, vol. 8, art. 100276, 2022, doi: 10.1016/j.jcomc.2022.100276.

[24] M. Elkolali, L. P. Nogueira, P. O. Ronning, and A. Alcocer, "Void content determination of carbon fiber reinforced polymers: A comparison between destructive and non-destructive methods," Polymers, vol. 14, no. 6, art. 1212, 2022, doi: 10.3390/polym14061212.

[25] X. Lu et al., "Accurate detection of porosity in glass fiber reinforced polymers by terahertz spectroscopy," Composites Part B: Engineering, vol. 242, art. 110058, 2022, doi: 10.1016/j.compositesb.2022.110058.

[26] W. Harizi, S. Chaki, G. Bourse, and M. Ourak, "Damage mechanisms assessment of glass fiber-reinforced polymer (GFRP) composites using multivariable analysis methods applied to acoustic emission data," Composite Structures, vol. 289, art. 115470, 2022, doi: 10.1016/j.compstruct.2022.115470.

[27] J. Jang, M. Maydison, Y. Kim, Z. Han, and D. Oh, "Effect of void content on the mechanical properties of GFRP for ship design," Journal of Marine Science and Engineering, vol. 11, no. 6, art. 1251, 2023, doi: 10.3390/jmse11061251.

[28] A. A. Abd-Elhady, A. Meroufel, H. E.-D. M. Sallam, and M. Atta, "Experimental and numerical determination of critical osmotic blister size affecting the strength of aged FRP seawater pipe," Polymers and Polymer Composites, vol. 29, no. 5, pp. 456-469, 2021, doi: 10.1177/0967391120922397.

[29] M. O. Ayanoglu, L. A. Carlsson, and E. Du, "Effects of void content on the moisture uptake and mechanical strength of a glass/epoxy composite," Journal of Composite Materials, vol. 57, no. 2, pp. 325-336, 2023, doi: 10.1177/00219983221144500.

[30] X. Yang, Y. Fang, R. Wang, Y. Li, and Z. Chen, "Visual quantitative detection of delamination defects in GFRP via microwave," Sensors, vol. 23, no. 14, art. 6386, 2023, doi: 10.3390/s23146386.

[31] Y. Zhang, Y. Li, X. Luan, B. Meng, J. Liu, and Y. Lu, "Effects of void characteristics on the mechanical properties of carbon fiber reinforced polyetheretherketone composites: Micromechanical modeling and analysis," Polymers, vol. 17, no. 13, art. 1721, 2025, doi: 10.3390/polym17131721.

[32] Y. K. Beng, M. N. Dalimin, and M. A. Faizal, "Mode-I toughness and curing pressure characteristic of symmetrical lay-up of plain-weave woven GFRP composites," Journal of Applied Sciences, vol. 7, no. 15, pp. 2174-2182, 2007, doi: 10.3923/jas.2007.2174.2182.

[33] T. S. Dawood, B. M. Fadhil, and D. O. Ramadan, "Effect of adding SiO2 nanoparticles on tensile and bending tests of glass/carbon hybrid composite materials," Journal of Jilin University (Engineering and Technology Edition), vol. 41, no. 11, pp. 55-68, 2022, doi:10.17605/OSF.IO/VCX68.

[34] T. W. Pribadi and R. C. Ariesta, "Study on Fiberglass Boat Strength and Durability under Different Types of Damage," in 2025 IEEE Ocean Engineering Technology and Innovation Conference: Management and Conservation for Sustainable and Resilient Marine and Coastal Resources (OETIC), Surabaya, Indonesia, 2025, pp. 163-169, doi: 10.1109/OETIC67587.2025.11512877.

[35] Biro Klasifikasi Indonesia, "Rules for Classification and Construction, Part 1 Seagoing Ships: Rules for Non-Metallic Materials," Jakarta, Indonesia, 2025.

[36] International Organization for Standardization, "ISO 527-1:2019, Plastics—Determination of tensile properties—Part 1: General principles," Geneva, Switzerland, 2019.

[37] International Organization for Standardization, "ISO 527-4:2021, Plastics—Determination of tensile properties—Part 4: Test conditions for isotropic and orthotropic fibre-reinforced plastic composites," Geneva, Switzerland, 2021.

[38] Standard Test Method for Tensile Properties of Plastics, ASTM D638-22, ASTM International, West Conshohocken, PA, USA, 2022, doi: 10.1520/D0638-22.

[39] M. M. Hiremath, T. Bernthaler, P. Anger, S. K. Mishra, A. Guha, And A. Tewari, “Comparison Of Damage Mechanisms In Chopped Strand Mat And Woven Roving Mat Composites Under Cyclic Tension,” *Polymer Composites*, Vol. 45, No. 12, Pp. 11162–11177, 2024, Doi: 10.1002/Pc.28539.

[40] R. Muharom, Alamsyah, T. Hidayat, and H. Syahab, "The Influence of Fiberglass Fiber Arrangement Variations on the Tensile and Bending Strength of Ships," Indonesian Journal of Maritime Technology, vol. 2, no. 2, pp. 57–67, 2024, doi: 10.35718/ismatech.v2i2.1203.

[41] M. U. Pawara et al., “Assessment of coconut petiole fiber-reinforced hybrid composites as sustainable materials for ship components,” Indonesian Journal of Maritime Technology, vol. 3, no. 2, pp. 142–149, 2025, doi: 10.35718/ismatech.v3i2.8481890.